Move-and-Charge System for Automatic Guided Vehicles

Chaoqiang Jiang[1], K. T. Chau[1], *Fellow, IEEE*, Chunhua Liu[2], Christopher H. T. Lee[3], Wei Han[1] and Wei Liu[1]

[1]Department of Electrical and Electronic Engineering, The University of Hong Kong, Hong Kong, China.
[2]School of Energy and Environment, City University of Hong Kong, Hong Kong, China.
[3]Research Laboratory of Electronics, Massachusetts Institute of Technology, MA, USA.

This paper proposes and implements a new move and charge (MAC) system for automatic guided vehicles (AGVs), which not only performs wireless charging, but also automatically navigates the AGV without using guiding sensors. The key is to make use of the DC-DC converter to maintain the equivalent load resistance, and then detect the charging current variation to conduct the desired traction under constant AC input current for the rail transmitter. In order to avoid frequent corrections of the forward direction and DC-DC converter regulation, both the straight rail and turning rail conditions are analyzed to determine the threshold value of the charging current. Without any misalignment, its transmission efficiency can reach up to 83% and the traction allowance can achieve up to 30 mm under the transmission distance of 80 mm. Both finite element analysis and experimental results are given to verify the validity of the proposed MAC AGV system.

***Index Terms*—Wireless power transfer, move and charge, automatic guided vehicles, auto navigation.**

I. Introduction

As one of the most prominent technologies [1], wireless power transfer (WPT) has attracted substantial attention in many applications such as wireless charging [2], wireless motoring [3, 4], wireless heating [5] and wireless lighting [6]. The WPT technique is changing the conventional usage of energy in daily life for human being [7]. Generally, the WPT system possesses the advantages of safety, reliability, low maintenance, and electrical isolation [8, 9], which are preferable by modern electric vehicles (EVs) [10, 11]. In recent years, the special EVs named automatic guided vehicles (AGVs) are highly demanded with the fast-increasing transportation and logistics market [12]. In order to alleviate the problem of their short driving range, more batteries or frequent charging are inevitable [13]. Rather than increasing the size of batteries or the number of charging ports, the use of WPT for AGVs can greatly facilitate the charging process [14].

Most importantly, because of the absence of metallic contacts, possible electrocution during the charging process can be totally eliminated [15]. Since the AGV usually needs to operate continuously, it is highly desirable to be wirelessly charged during moving. Namely, an array of power transmitters is embedded beneath the workplace while a receiver is mounted at the bottom of the AGV. Another problem for AGV application is that it desires a large number of sensors embedded under the workplace to navigate these AGVs, which will significantly increase the system complexity and hardware cost.

This paper proposes and implements a new move-and-charge (MAC) system for AGVs. Essentially, the proposed rail transmitter not only serves to wirelessly charge the AGV, but also to navigate the AGV based on the variation of mutual inductance. Thus, it can significantly reduce the battery size, while eliminating the risk of electrocution and the guiding sensors embedded under the workplace. The key is to make use of the DC-DC converter to keep the equivalent resistance constant [16]. When the AGV is misaligned with the rail transmitter, the receiver current will be varied so that the steering part of the AGV will perform the correction of direction to maintain the received power. Consequently, both dynamic charging and navigation can be achieved simultaneously. By using finite element analysis (FEA), the corresponding magnetic field distributions and reference current will be analyzed at different aligned positions. Also, experimental results will be given to verify the proposed MAC AGV system.

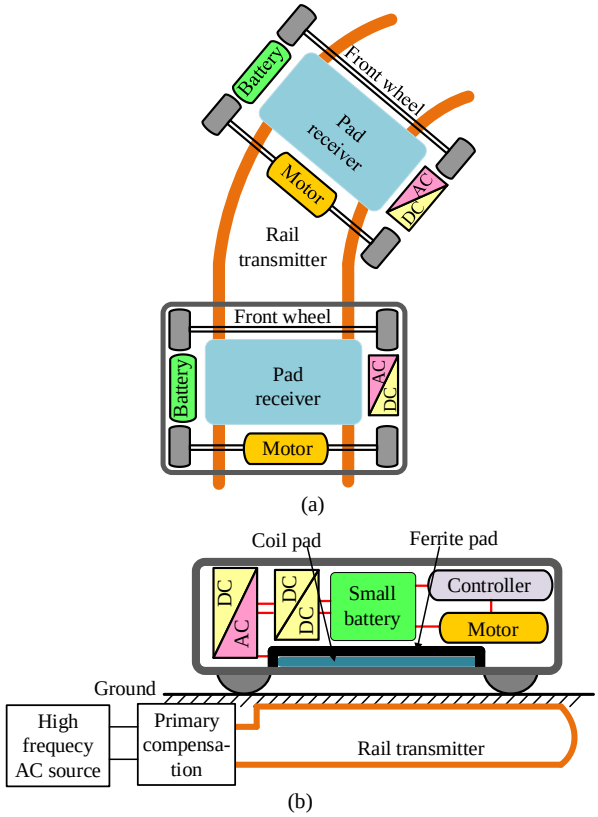

Fig. 1. Proposed MAC AGV system: (a) Schematic. (b) System structure.

Manuscript received ; revised and; accepted . Date of publication ; date of current version. Corresponding author: K. T. Chau (e-mail: ktchau@eee.hku.hk).

II. System Configuration and Operation

A. System Configuration

The proposed MAC AGV system is shown in Fig. 1(a), which includes the rail transmitter designed with 180 mm width and the pad receiver. The rail transmitter is embedded just beneath the ground while the pad receiver is mounted at the bottom of the AGV so that the airgap between them is 80 mm. The rail transmitter design involves only a long primary coil supplied by a single power inverter, which takes the definite advantages of lower investment cost and lower installation complexity than the pad transmitter design for feeding multiple AGVs.

For the sake of better flexibility, maintainability and scalability, the rail transmitter design usually adopts the sectional arrangement in which it uses one power inverter per section to feed multiple AGVs. Normally, the rail transmitter should be compensated with capacitors as shown in Fig. 1(b), and the system operation frequency is set at 85 kHz according to the SAE J2954 wireless charging standard. Since the wireless power from the transmitter to the receiver is proportional to the surface area where the magnetic flux passes through, the ferrite based pad receiver is adopted to provide magnetic flux guidance, hence minimizing the flux leakage.

In order to provide the effect of navigation without relying on guiding sensors, the DC-DC converter is used to regulate the charging voltage and current, aiming to keep the equivalent resistance constant. If the AGV is not aligned with the rail transmitted, there will be a difference between the received current and reference current. Although different curvatures of rail can produce different alignments for the same induced current drop, the direction correction still can be effectively achieved based on the current threshold control. This difference will cause the steering part of the AGV to control the AGV in such a way that the alignment can be restored.

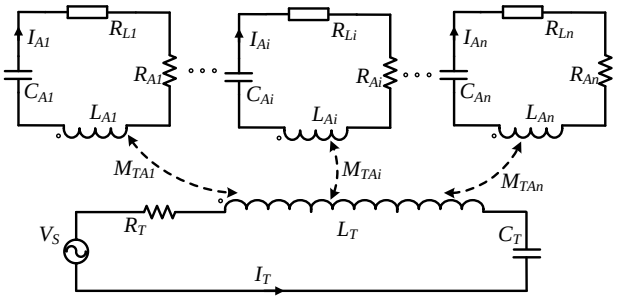

Fig. 2. Equivalent circuit of MAC multiple-AGV system.

B. WPT Operation

For the proposed MAC AGV system with multiple AGVs, the simplified equivalent circuit is shown in Fig. 2. The system involves the AC input voltage V_S, the compensated capacitor C_T, several AGV receivers with the inductance L_{Ai} and equivalent load resistance R_{Li}, in which R_T, L_T are the resistance and inductance of the rail transmitter coil, C_{Ai} and R_{Ai} are the capacitance and resistance of each AGV receiver coil, I_T and I_{Ai} are the currents of the rail transmitter and each receiver, and M_{TAj} is the mutual inductance between the rail transmitter coil and each receiver coil. The mutual inductances between two AGV receiver coils are ignored because they are arranged on the same plane. When the rail transmitter is operated with constant input current, the input voltage V_S will increase with the increase of AGV number due to the increased reflected resistance from each receiver. Generally, the system equation can be express as

$$\begin{bmatrix} j(\omega L_T - 1/(\omega C_T)) + R_T & j\omega M_{TA1} & \cdots & j\omega M_{TAn} \\ j\omega M_{TA1} & Z_{A1} + R_{L1} & \cdots & 0 \\ \vdots & \vdots & \ddots & \vdots \\ j\omega M_{TAn} & 0 & 0 & Z_{An} + R_{Ln} \end{bmatrix} \cdot \begin{bmatrix} \boldsymbol{I_T} \\ \boldsymbol{I_{A1}} \\ \vdots \\ \boldsymbol{I_{An}} \end{bmatrix} = \begin{bmatrix} \boldsymbol{V_S} \\ \boldsymbol{0} \\ \boldsymbol{0} \\ \boldsymbol{0} \end{bmatrix} \tag{1}$$

where ω represents the operating frequency, and Z_{Ai} is the resultant reactance in the receiver i ($i=1,2,\ldots,n$) which is equal to $j(\omega L_{Ai} - 1/(\omega C_{Ai}) + R_{Ai}$.

In order to evaluate the power transfer ability of the transmitter, the apparent power of the transferred energy S_T relies on the reflected impedances to the transmitter, which can be given by

$$S_T = I_T{}^2 Z_{AT} \tag{2}$$

where Z_{AT} is the total reflected impedances for all AGV receivers to the transmitter part. It can be obtained as

$$Z_{AT} = \sum_{i=1}^{n} \frac{-j\omega M_{TAi} I_{Ai}}{I_T} = \sum_{i=1}^{n} \frac{\omega^2 M_{TAi}{}^2}{Z_{Ai} + R_{Li}} \tag{3}$$

As a result, the AC input voltage V_S can be calculated by

$$V_S = I_T\left(j\left(\omega L_T - \frac{1}{\omega C_T}\right) + R_T + Z_{AT}\right) \tag{4}$$

Thus, the operation frequency ω should be the same with the resonant frequency of the transmitter to maximum the transferred power S_T and reduce the AC input voltage V_S. Meanwhile, all AGV receivers should be tuned to the same resonant frequency of the transmitter.

When the rail transmitter is operated with constant current, then the output current for a single AGV I_{Ai} and the received power P_{Ai} can be expressed as

$$\begin{cases} I_{Ai} = \dfrac{j\omega M_{TAi} I_T}{Z_{Ai} + R_{Li}} \\ P_{Ai} = \dfrac{\omega^2 M_{TAi}{}^2 I_T{}^2}{(Z_{Ai} + R_{Li})^2} R_{Li} \end{cases} \tag{5}$$

As a result, the system transmission efficiency and power transfer ability can be written by

$$(I_{Ai}, P_{Ai}) = f(\omega, R_{Li}, M_{TAi}) \tag{6}$$

For exemplification, the key parameters are listed in TABLE I. The charging current and power can be calculated with respect to different mutual inductances and equivalent load resistances. As depicted in Fig. 3, it can be observed that both the AGV charging current and power increase with the increase of mutual inductance. Also, the charging current decreases with the increase of the load resistance. When the AGV pad receiver is not centrally aligned with the rail transmitter, the mutual inductance will be varied. Thus, by sensing the charging current, the AGV can effective detect the

position variation and then conduct the correction of forward direction. Moreover, by selecting a threshold value, which is slightly lower than the centrally aligned charging current, both the equivalent load and position will achieve some proper allowance to avoid frequent corrections of the forward direction and DC-DC converter regulation.

TABLE I. System parameters

Item	VALUE	Unit
Resonant frequency (f)	85	kHz
Current of transmitter (I_T)	4.5	A
Resistance of transmitter coil (R_T)	1.2	Ω
Resistance of receiver coil (R_{Aj})	0.4	Ω
Inductance of transmitter (L_T)	0.55	mH
Inductance of receiver (L_{Ri})	0.2	mH
Compensation of transmitter (C_T)	6.37	nF
Compensation of receiver (C_{Ai})	17.5	nF

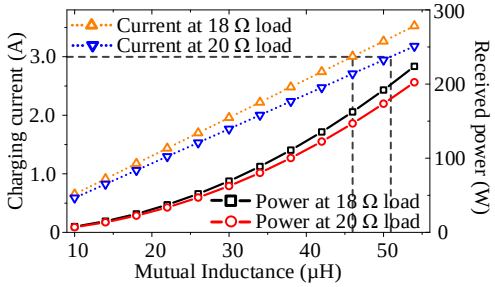

Fig. 3. Calculated charging current and power at different mutual inductances.

III. SIMULATION AND ANALYSIS

In order to predefine the abovementioned reference current, the magnetic field distributions at different situations are calculated by using FEA based software JMAG. Generally, the total effective flux passes through the pad receiver can be used to reflect the charging current or power transmission ability. For quantitively analyze the magnetic field distribution at various misalignments, a 200 W MAC AGV system has been adopted under the constant input current of 2.1 A for the rail transmitter.

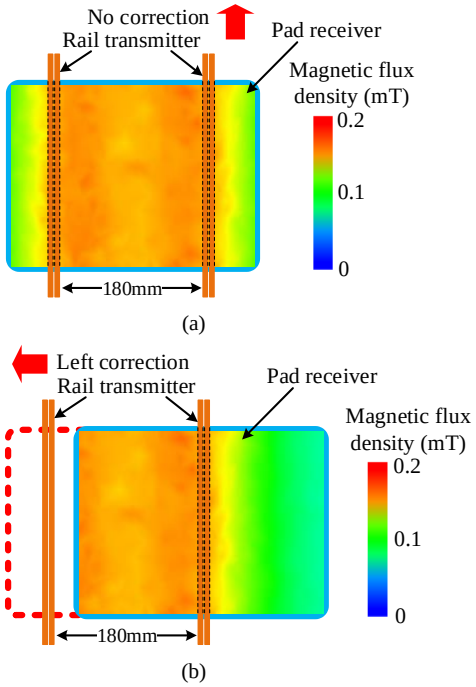

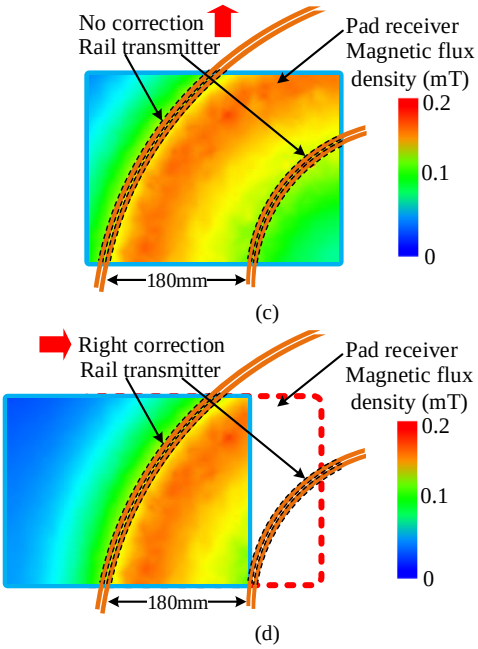

Fig. 4. Simulation results of magnetic flux density distribution at the height of 80 mm. (a) Above straight rail without correction. (b) Above straight rail with left correction. (c) Above turning rail without correction. (d) Above turning rail with right correction.

As shown in Fig. 4(a), when the pad receiver of the AGV is exactly aligned with the rail transmitter, the magnetic flux density at the height of 80 mm is symmetrical without requiring any correction of direction. Once the AGV is off tracking the rail transmitter, the total effective flux passes through the pad receiver is reduced, as shown in Fig. 4(b), and then the left correction will be needed to eliminate the misalignment. Meanwhile, when the AGV comes across the right turning rail, the aligned magnetic flux density is shown in Fig. 4(c). Also, the right correction is needed when the AGV detects the reduced current, which is caused by the reduce of passed through magnetic flux as shown in Fig. 4(d).

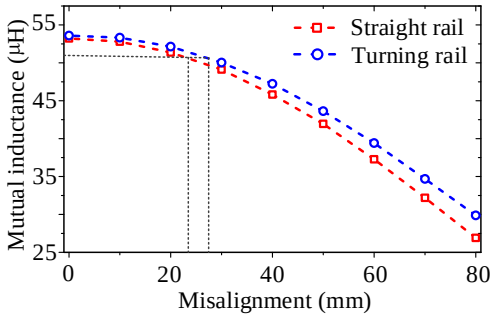

Fig. 5. Mutual inductance variation with respect to various misalignments at different rail positions.

Moreover, it should be noticed that the effective flux through areas of the centrally aligned straight and turning rails are slightly different due to the arc shape. As shown in Fig. 5, the aligned mutual inductance of straight and turning rails are 52.8 μH and 53.6 μH, respectively. And then both drop fast with respect to the misalignment. According to the reduction of mutual inductance, the charging current of the pad receiver is reduced correspondingly as shown in Fig. 6. It can be observed that the current density of pad receiver at centrally

aligned position is larger than that at the misalignment of 50 mm. All these simulation results confirm that the proposed system can possess the wireless charging and the AGV misalignment correction simultaneously.

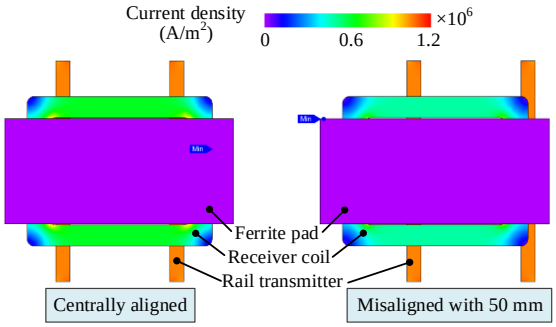

Fig. 6. Current density distributions at centrally aligned and misaligned positions.

IV. Experimental Validation

An experimental prototype has been constructed as shown in Fig. 7, in which the programmable function generator (AFG3000C) is used to drive the wideband power amplifier (EI1000S04) to produce the desired AC power, the oscilloscope (Lecroy 6100A) is used to measure voltages and then calculate the efficiency, the currents are measured by (AM503B), and the mutual inductance is measured by the LCR meter (ISO-TECH LCR821). The operation frequency is set at 84.5 kHz due to the practical parameters.

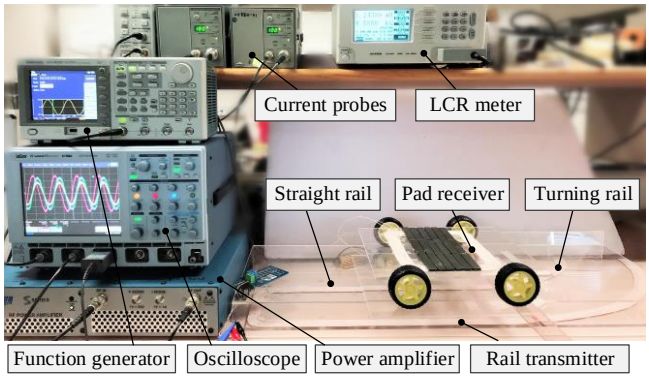

Fig. 7. Experimental setup of the proposed MAC AGV system.

For experimentation, the testing input power is scaled down to 80 W and the transmission airgap is set at 80 mm. As shown in Fig. 8, both the measured mutual inductances of the straight and turning rail decrease with the increase of misalignment. Also, the mutual inductance above the turning rail is slightly higher than that above the straight rail, which is well agree with the FEA simulation result. Moreover, the centrally aligned charging current can reach 2.35 A as shown in Fig. 9(a) whereas the charging current with 50 mm misalignment is only 1.79 A as shown in Fig. 9(b). Furthermore, the corresponding charging current and transmission efficiency are measured as shown in Fig. 10. It can be found that both current and efficiency decrease with the increase of misalignment. Thus, when the reference current of 2.25 A is set as the threshold value to conduct the direction correction, the correction allowances above the straight and turning rail can achieve 20 mm and 30 mm, respectively.

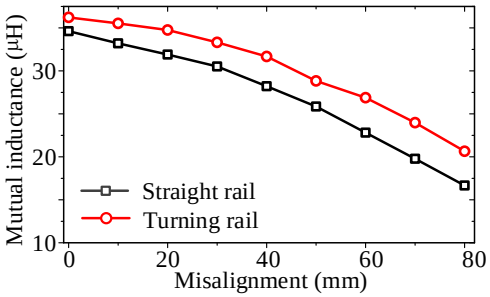

Fig. 8. Measured mutual inductance variation with respect to various misalignments.

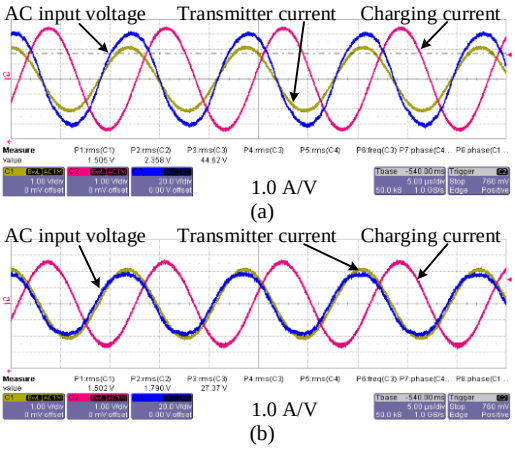

Fig. 9. Measured current waveforms above the straight rail. (a). Centrally aligned. (b). With misalignment of 50 mm.

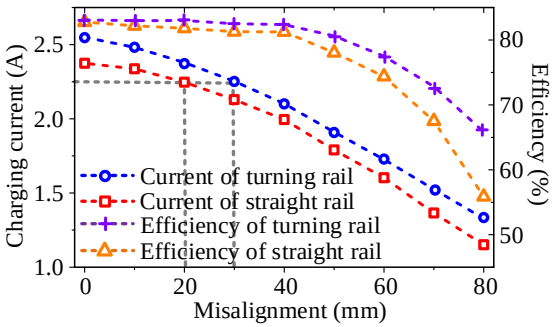

Fig. 10. Measured currents and transmission efficiencies with respect to different misalignments.

V. Conclusion

In this paper, a new MAC system has been proposed and implemented for AGVs, which not only performs wireless charging, but also automatically navigates the AGV without using guiding sensors. By newly adopting the equivalent resistance adjustment and current threshold control method, it can simultaneously provide wireless power and misalignment correction, hence achieving the desired traction. Most importantly, it can significantly reduce the battery size and hence cost of each AGV, while eliminating the risk of electrocution. Both finite element analysis and experimental results can well verify the validity of the proposed MAC AGV system. In particular, the measured transmission efficiency and traction allowance can achieve up to 83% and 30 mm, respectively.

ACKNOWLEDGMENT

This work was supported by a grant (Project No. 17204317) from the Hong Kong Research Grants Council, Hong Kong Special Administrative Region, China.

REFERENCES

[1] G. A. Covic, and J. T. Boys, "Inductive power transfer," *Proceedings of the IEEE*, vol. 101, no. 6, pp. 1276-1289, Jun, 2013.

[2] C. C. Mi, G. Buja, S. Y. Choi, and C. T. Rim, "Modern advances in wireless power transfer systems for roadway powered electric vehicles," *IEEE Transactions on Industrial Electronics*, vol. 63, no. 10, pp. 6533-6545, Oct, 2016.

[3] C. Jiang, K. T. Chau, C. Liu, and W. Han, "Design and analysis of wireless switched reluctance motor drives", *IEEE Transactions on Industrial Electronics*, DOI: 10.1109/TIE.2018.2829684.

[4] C. Jiang, K. T. Chau, C. Liu, and W. Han, "Wireless DC motor drives with selectability and controllability," *Energies*, vol. 10, no. 1, pp. 49:1-15, Jan. 2017.

[5] W. Han, K.T. Chau, Z. Zhang, and C. Jiang, "Single-source multiple-coil homogeneous induction heating," *IEEE Transactions on Magnetics*, vol. 53, no. 11, pp. 7207706:1-6, Nov, 2017.

[6] C. Jiang, K. T. Chau, Y. Y. Leung, C. Liu, C. H. T. Lee, and W. Han, "Design and analysis of wireless ballastless fluorescent lighting", *IEEE Transactions on Industrial Electronics*, DOI: 10.1109/TIE.2017. 2784345.

[7] A. P. Sample, D. T. Meyer, and J. R. Smith, "Analysis, experimental results, and range adaptation of magnetically coupled resonators for wireless power transfer," *IEEE Transactions on Industrial Electronics*, vol. 58, no. 2, pp. 544-554, Feb, 2011

[8] C. Jiang, K. T. Chau, C. Liu, and C. H. T. Lee, "An overview of resonant circuits for wireless power transfer," *Energies*, vol. 10, no. 7, pp. 894:1-20, Jun, 2017.

[9] Z. Zhang, K. T. Chau, C. Liu, F. Li, and T.W. Ching, "Quantitative analysis of mutual inductances for optimal wireless power transfer via magnetic resonant coupling," *IEEE Transactions on Magnetics*, vol. 50, no. 11, pp. 8600504:1-4, Nov, 2014.

[10] C. Jiang, K. T. Chau, T. W. Ching, C. Liu, and W. Han, "Time-division multiplexing wireless power transfer for separately excited DC motor drives", *IEEE Transactions on Magnetics*, vol. 53, no. 11, pp. 1-5, Nov, 2017.

[11] K. T. Chau, C. Jiang, and W. Han, "State-of-the-art electromagnetics research in electric and hybrid vehicles", *Progress in Electromagnetics Research*, vol. 159, pp. 139-157, Oct, 2017.

[12] A. Vale, R.Ventura, P. Lopes, and I. Ribeiro, "Assessment of navigation technologies for automated guided vehicle in nuclear fusion facilities," *Robotics and Autonomous Systems*, vol. 97, pp. 153-170, Nov., 2017.

[13] C. Qiu, K. T. Chau, C. Liu, T. W. Ching, and Z. Zhang, "Modular inductive power transmission system for high misalignment electric vehicle application," *Journal of Applied Physics*, vol. 117, no. 17, pp. 17B528:1-4, Apr, 2015.

[14] M. H. Mahmud, W. Elmahmoud, M. R. Barzegaran, and N. Brake, "Efficient wireless power charging of electric vehicle by modifying the magnetic characteristics of the transmitting medium," *IEEE Transactions on Magnetics*, vol. 53, no. 6, pp. 1-5, Jan., 2017.

[15] Y. Bu, T. Mizuno, and H, Fujisawa, "Proposal of a wireless power transfer technique for low-power multireceiver applications," *IEEE Transactions on Magnetics*, vol. 51, no. 11, pp. 1-4, Nov, 2015.

[16] T. D. Yeo, D. S. Kwon, S. T. Khang, and J. W. Yu, "Design of maximum efficiency tracking control scheme for closed-loop wireless power charging system employing series resonant tank," *IEEE Transactions on Power Electronics*, vol. 32, no. 1, pp. 471-478, Jan, 2017.